AFRL-AFOSR-VA-TR-2021-0065

Molecular Engineering of Hybrid Perovskites Quantum Wells for Nano-Photonics

Xu, Xiaodong
UNIVERSITY OF WASHINGTON
4333 BROOKLYN AVE NE
SEATTLE, WA, 98195
USA

07/02/2021
Final Technical Report

Air Force Research Laboratory
Air Force Office of Scientific Research
Arlington, Virginia 22203
Air Force Materiel Command

REPORT DOCUMENTATION PAGE

Form Approved
OMB No. 0704-0188

1. REPORT DATE *(DD-MM-YYYY)*	**2. REPORT TYPE**	**3. DATES COVERED** *(From - To)*
02-07-2021	Final	01 Dec 2017 - 14 Dec 2020

4. TITLE AND SUBTITLE
Molecular Engineering of Hybrid Perovskites Quantum Wells for Nano-Photonics

5a. CONTRACT NUMBER

5b. GRANT NUMBER
FA9550-18-1-0046

5c. PROGRAM ELEMENT NUMBER
61102F

6. AUTHOR(S)
Xiaodong Xu

5d. PROJECT NUMBER

5e. TASK NUMBER

5f. WORK UNIT NUMBER

7. PERFORMING ORGANIZATION NAME(S) AND ADDRESS(ES)
UNIVERSITY OF WASHINGTON
4333 BROOKLYN AVE NE
SEATTLE, WA 98195
USA

8. PERFORMING ORGANIZATION REPORT NUMBER

9. SPONSORING/MONITORING AGENCY NAME(S) AND ADDRESS(ES)
AF Office of Scientific Research
875 N. Randolph St. Room 3112
Arlington, VA 22203

10. SPONSOR/MONITOR'S ACRONYM(S)
AFRL/AFOSR RTB2

11. SPONSOR/MONITOR'S REPORT NUMBER(S)
AFRL-AFOSR-VA-TR-2021-0065

12. DISTRIBUTION/AVAILABILITY STATEMENT
A Distribution Unlimited: PB Public Release

13. SUPPLEMENTARY NOTES

14. ABSTRACT

Breakthroughs in science and technologies often come with the discovery of new material systems with advancement in synthesis methods. An outstanding example is the development of quantum wells (QWs) and heterostructures made of three dimensional semiconductors, which have provided the foundation for repeated breakthroughs in key solid-state device technologies, such as light-emitting diodes, diode lasers, photovoltaics and many optoelectronic components. The goal of this project is to elucidate the processing, structure, function relationships of two-dimensional (2D) layered perovskites and their heterostructures to enable them to serve as advanced optoelectronic materials. 2D layered perovskites represent a new class of low-dimensional semiconductors that offer unprecedented possibilities for technological applications in nanoelectronics and nanophotonics, which can be used by Air Force to improve our national securities and peacekeeping capabilities.

The advantages of 2D hybrid layered perovskites arise from their intrinsic material structure, which comprises alternating organic and inorganic layers to form an extended ordered structure naturally. The organic and inorganic parts in such hybrid perovskites contributes very differently to the overall physical properties of the material, permitting one to separately tune the organic and inorganic contributions to the overall optoelectronic properties, but also making the chemistry, processing, and function relationship of 2D layered perovskites subtly different from either purely organic or purely inorganic materials. In this project, we have systematically studied the effect of organic spacer cations on the optoelectronic properties and device performance using the 2D layered perovskites. We observed that both larger and more hydrophobic organic cations can improve perovskite stability against moisture, while larger size can adversely influence the device performance. Organic spacer ligands with aromatic moieties such as naphthalene, pyrene, or perylene have been demonstrated to enhance the out-of-plane conductivity and photovoltaic performance. We have introduced all aromatic delocalized cations into the quasi-2D perovskites also. The resulting perovskites show enhanced hole and electron mobilities and subsequently improved performance compared to the well-known organic cation PEAI-based quasi-2D perovskites. Moreover, we have developed post-synthesis modification based on molecular exchange of organic cations that allow surface doping and modification of organic layers of 2D hybrid perovskites. Furthermore, we have discovered a novel series of organic cations with N-methyl ammonium as a new cationic functional group persistently interacting with layered inorganic layers. We expect these findings will enable the development of complex QW device structures with greater flexibility in material structural engineering over MBE technologies.

15. SUBJECT TERMS

16. SECURITY CLASSIFICATION OF:			**17. LIMITATION OF ABSTRACT**	**18. NUMBER OF PAGES**	**19a. NAME OF RESPONSIBLE PERSON**
a. REPORT	**b. ABSTRACT**	**c. THIS PAGE**			KENNETH CASTER
U	U	U	UU	27	**19b. TELEPHONE NUMBER** *(Include area code)*

Final Report for AFOSR-FA9550-18-1-0046

Program Manager: Dr. Kenneth Caster

Project Title:

Molecular Engineering of Hybrid Perovskites Quantum Wells for Nano-Photonics

Principal Investigator: Xiaodong Xu
Co-Principal Investigator: Alex K-Y. Jen
Department of Materials Science & Engineering, University of Washington

Reporting Period:

12/15/2017-12/14/2020

Technical Contact:
Xiaodong, Xu
Professor
Department of Physics,
Department of Materials Science and Engineering
University of Washington
Seattle, WA 98195-3150
(206)543-8444
xuxd@uw.edu

Administrative/Business Contact:
Amanda Snyder
4333 Brooklyn Avenue, NE
Seattle, WA 98195-9472
Phone:206-543-4043
Fax:206-685-1732
Email: osp@u.washington.edu

Abstract

Breakthroughs in science and technologies often come with the discovery of new material systems with advancement in synthesis methods. An outstanding example is the development of quantum wells (QWs) and heterostructures made of three dimensional semiconductors, which have provided the foundation for repeated breakthroughs in key solid-state device technologies, such as light-emitting diodes, diode lasers, photovoltaics and many optoelectronic components. The goal of this project is to elucidate the processing, structure, function relationships of two-dimensional (2D) layered perovskites and their heterostructures to enable them to serve as advanced optoelectronic materials. 2D layered perovskites represent a new class of low-dimensional semiconductors that offer unprecedented possibilities for technological applications in nanoelectronics and nanophotonics, which can be used by Air Force to improve our national securities and peacekeeping capabilities.

The advantages of 2D hybrid layered perovskites arise from their intrinsic material structure, which comprises alternating organic and inorganic layers to form an extended ordered structure naturally. The organic and inorganic parts in such hybrid perovskites contributes very differently to the overall physical properties of the material, permitting one to separately tune the organic and inorganic contributions to the overall optoelectronic properties, but also making the chemistry, processing, and function relationship of 2D layered perovskites subtly different from either purely organic or purely inorganic materials. In this project, we have systematically studied the effect of organic spacer cations on the optoelectronic properties and device performance using the 2D layered perovskites. We observed that both larger and more hydrophobic organic cations can improve perovskite stability against moisture, while larger size can adversely influence the device performance. Organic spacer ligands with aromatic moieties such as naphthalene, pyrene, or perylene have been demonstrated to enhance the out-of-plane conductivity and photovoltaic performance. We have introduced all aromatic delocalized cations into the quasi-2D perovskites also. The resulting perovskites show enhanced hole and electron mobilities and subsequently improved performance compared to the well-known organic cation PEAI-based quasi-2D perovskites. Moreover, we have developed post-synthesis modification based on molecular exchange of organic cations that allow surface doping and modification of organic layers of 2D hybrid perovskites. Furthermore, we have discovered a novel series of organic cations with N-methyl ammonium as a new cationic functional group persistently interacting with layered inorganic layers. We expect these findings will enable the development of complex QW device structures with greater flexibility in material structural engineering over MBE technologies.

1 Motivation of the work

The development of quantum wells (QWs) and heterostructures made of three-dimensional semiconductors, which have provided the foundation for repeated breakthroughs in key present-day solid-state technologies, such as light-emitting diodes, diode lasers, photovoltaics and many optoelectronic components. Two-dimensional (2D) layered perovskites represent a new class of low-dimensional semiconductors that offer unprecedented possibilities for technological applications in nanoelectronics and photonics, which can be used by Air Force to improve our national warfighting and peacekeeping capabilities. Compared to QWs and heterostructures formed by 3D semiconductors, layered perovskites offer greater tunability in material properties and possibilities for cheaper and faster synthesis through chemical means such as solution- and vapor-based growth processes. These advantages of 2D hybrid layered perovskites arise from their intrinsic material structure, which comprises alternating organic and inorganic layers to form a naturally long-range ordered structure. The organic and inorganic parts in such hybrid perovskites contributes very differently to the overall physical properties of the material, permitting one to separately tune the organic and inorganic contributions to the overall optoelectronic properties, but also making the chemistry, processing, and function relationship of 2D layered perovskites subtly different from either purely organic or purely inorganic materials.

2. Objective

The goal of this project is to elucidate the processing, structure, function relationships of 2D layered perovskites and their heterostructures to enable the development of advanced optoelectronic and photonic applications. Specific aims include establishing design relationships between structural parameters, quantum confinement, and optoelectronic properties of both type I and type II hybrid 2D perovskite QWs; developing post-synthesis modifications that allow surface doping, modification, and molecular exchange of either deposited inorganic or organic domains; employing a suit of tools to investigate how structure controls the fundamental electronic and optical properties of these perovskite QWs and heterostructures, including interfacial energy level alignment, excitonic properties, and nonlinear optical properties.

3. Progress Summary

During this award, we have made significant progress towards developing rational design and synthesis of 2D hybrid perovskite quantum well structures, and understanding its light matter interactions. Specific achievements include:

- Establish design relationships between structural parameters, quantum confinement, and optoelectronic properties of hybrid 2D perovskite QWs (both single and double QWs).
- Demonstrate and explore these relationships within both type I and type II 2D perovskite heterostructures created by co-assembly of differing inorganic layers as well as combinations of semiconducting organic species, inorganic sheets, and surface-templated patterning to enable direct growth on device relevant substrates.
- Develop post-synthesis modifications that allow surface doping, modification, and molecular exchange of either deposited inorganic or organic domains.
- Employ a wide range of techniques to investigate how structure controls the fundmental electronic and optical properties of these perovskite QWs and heterotructures, including properties such as interfacial energy level alignment, excitonic properties (lifetime, drift-diffusion, binding energy etc.), electro-optical properties, nonlinear optical properties as a function of electrostatic control, and many-body interaction effects such as Auger scattering.

4. Brief Description of Technical Progresses

The recent emergence of a new class of hybrid layered perovskites, offers a great opportunity for transformational breakthrough in electronic and photonic technologies. One of the major goal of this project is to develop structure/property relationships of 2D layered perovskites and their heterostructures to enable them to function as advanced optoelectronic materials. Specific aims include:

- Establish relationships between structural parameters, quantum confinement, and optoelectronic properties of hybrid 2D perovskite QWs (both single and double QWs (**Figure 1a-1b**));
- Demonstrate and explore these relationships within both type I and type II 2D perovskite heterostructures (**Figure 1c**) created by co-assembly of differing inorganic layers and combinations of semiconducting organic species, inorganic sheets, and surface-templated patterns of these heterostructures directly on device relevant substrates;
- Develop post-synthesis modifications of the heterostructures to enable surface doping, and molecular exchange of deposited inorganic or organic domains;

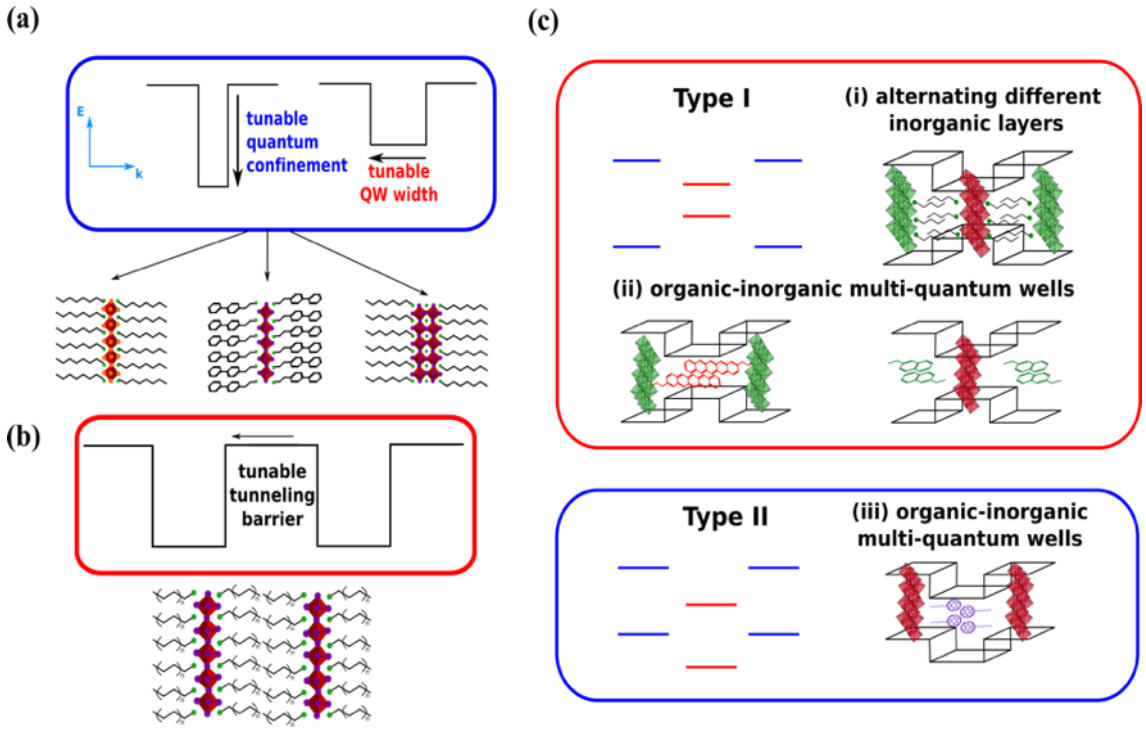

Figure 1. 2D hybrid perovskite QW structures developed through this project: (a) single quantum well, (b) symmetric double quantum well, and (c) heterostructured double quantum well with schematic representations of the prioritized heterostructures for light emission (type I) and energy transport (type II). Here the red inorganic layer has a smaller bandgap than the green layer.

Compared to the compositional restrictions of the 3D hybrid materials, 2D layered perovskites afford a greater degree of innovation and flexibility in design due to the larger size tolerance in the third dimension. In 2D layered perovskites, alternating organic and inorganic layers form a long-range ordered structure. Generally, the organic and inorganic parts in such

perovskites contribute very differently to the overall band structure and chemical properties, thereby allowing each domain to be separately varied to tune their optoelectronic properties. More importantly, the 2D layered perovskites can accommodate much simpler, cost effective, and scalable synthetic processes.

Synthetic flexibility of molecular compositions provides diverse potential innovations in the design of 2D layered perovskite. In the case of insulating aliphatic organic domains, metal halide layers provide "an energetic well" with organic layers serving as the potential barriers. Tunneling between these wells can be easily tuned by modifying aliphatic chain length and dielectric constant, which can also be utilized to shift the associated exciton binding energy. The structure and molecular packing of the organic species affect the crystal and electronic structure of inorganic layer and enhance the overall diversity of hybrid functionality. By incorporating semiconducting functionality into organic domains, organic-inorganic hybrid QWs and multilayer heterostructures can also be realized also. Therefore, frontier energy levels as well as molecular packing and doping of the organic semiconductor layers can be engineered systematically to tune the resulting opto-electronic properties of 2D perovskites for specific device applications. Results from these areas of progress are summarized in more detail below.

4.1 <u>Incorporation of additives for morphological control of multidimensional hybrid perovskites</u>: The use of 2D or quasi-2D perovskite structures is one of the most effective and commonly used methods for achieving improved material stability. The quasi-2D perovskites with a structure of $(RNH_3)_2A_{n-1}Pb_nX_{3n+1}$ (R is an aromatic or aliphatic alkylammonium cation, A is $CH_3NH_3^+$ or $HC(NH_2)_2^+$, X is a halide ion, and n defines the layer number of the perovskite sheets) with low n values exhibit enhanced ambient stability, which has inspired their use as replacements for the 3D perovskites. However, these improvements in stability have been compensated by decreased performance due to reduced charge transport between the sheets caused by the long organic spacing ligand. To address this issue, several strategies had been applied to orient the quasi-2D perovskite vertically along the carrier collection direction to electrodes, including hot-casting deposition, processing with additives, adopting shorter spacer ligands, and incorporating FA^+ cation or Cs^+ cation, which have improved the PCE of stable, quasi-2D ($n < 5$) perovskite solar cells (PVSCs) to 13.7%.

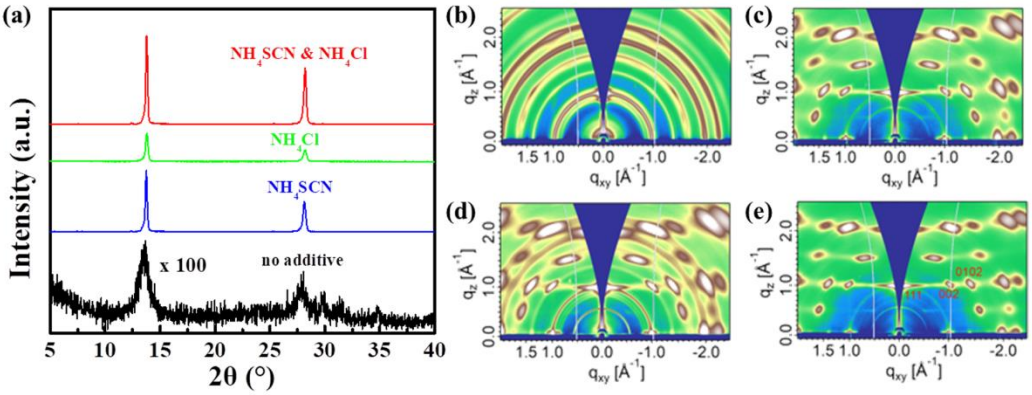

Figure 2. Crystallinity and structural orientation. (a) X-ray diffraction patterns of the perovskite films fabricated with various additives. GIWAXS maps for perovskite films fabricated with various additives: (b) without additive; (c) NH_4SCN as additive; (d) NH_4Cl as additive and (e) NH_4SCN and NH_4Cl as additives.

Despite of consistently improving charge transport and short-circuit current densities with these materials, little attention has been paid to alleviate the high levels of non-radiative recombination present in these films. As a result, quasi-2D PVSCs suffer a non-radiative open-circuit voltage (V_{OC}) loss ($V_{non\text{-}rad} = V_{SQ\text{-}limit} - V_{OC}$) of ~ 0.22-0.6 V, with $V_{SQ\text{-}limit}$ representing the V_{OC} upper limit for absorbers under Schockley-Queisser limit. As a comparison, the optimized 3-D perovskite systems can show a non-radiative V_{OC} loss as low as ~ 0.1 V.

We have demonstrated highly efficient quasi 2D PVSCs by simultaneously incorporating NH_4SCN and NH_4Cl as additives. We find that NH_4SCN and NH_4Cl can enhance the crystallinity of quasi-2D perovskite $(PEA)_2(MA)_4Pb_5I_{16}$ film and induce preferential orientation of the (0k0) planes perpendicular to the electrode, as evidenced by X-ray diffraction (XRD) and grazing incidence wide-angle X-ray scattering (GIWAX) measurements (**Figure 2**). The perovskite films were fabricated using a one-step coating method. Typically, a mixture of phenylethylammonium iodide (PEAI), methylammonium iodide (MAI), PbI_2, and processing additive (NH_4SCN and/or NH_4Cl) were dissolved in *N*,*N*-dimethylformamide (DMF) at a concentration of 1.0 M, and the solution was then spin-coated onto a PEDOT:PSS substrate. The film without additives shows very low crystallinity, as indicated by the weak and broad peaks at about 14° and 28° that correspond to the (111) and (202) facets of 2D perovskites. After additives are added, these two diffraction peaks show enhanced intensity (with a factor of 35–110) and also a narrowed full width at half-maximum (FWHM). In particular, the FWHM of the peak at $2\theta = 14°$ decreases from 0.641° (without additive) to 0.266° (with NH_4Cl), 0.208° (with NH_4SCN), and 0.205° (with both NH_4Cl and NH_4SCN). These results indicate that both the NH_4SCN and NH_4Cl additives can increase the crystallinity of the 2D perovskite films, with NH_4SCN having a stronger effect, and that the simultaneous addition of NH_4SCN and NH_4Cl produces the film with the highest crystallinity.

The growth of quasi-2D perovskite films with excellent crystallinity, preferred orientation, and high uniformity is favorable for exploring their use in planar photovoltaic devices. Planar-structured PVSCs with the device structure of ITO/PEDOT:PSS/$(PEA)_2(MA)_4Pb_5I_{16}$/$PC_{61}BM$/BCP/Ag were fabricated. We found the addition of NH_4Cl improves the V_{OC} from 1.11 V (with only NH_4SCN additive) to 1.21 V, with the electroluminescence external quantum efficiency (ELQE) improving from 0.1% for NH_4SCN-only films to 0.68% at + 2.5 V bias. When both NH_4SCN and NH_4Cl were added, we observed that devices benefit from the combined additives, exhibiting a high V_{OC}, J_{SC}, and FF of 1.21 ± 0.01 V, 15.2 ± 0.6 mA cm^{-2}, and 0.70 ± 0.02, respectively, at a NH_4SCN/NH_4Cl molar ratio of 1:1. Together, these measurements confirm the achievement of record-low non-radiative V_{OC} loss of ~ 0.16 V for quasi-2D systems. The planar-structured PVSCs with both additives exhibit an average and champion PCE of 12.9 ± 0.8% and 14.1%, respectively, which is among the highest reported PCEs for quasi-2D systems. We further conduct Glow Discharge Optical Emission Spectroscopy (GDOES) depth profiling, internal quantum efficiency (IQE) and photoluminescence (PL) measurements, and drift-diffusion simulation to reveal that the reduced non-radiative recombination originates from a Cl^- passivation of electron traps near the PEDOT:PSS/perovskite hole-collecting interfaces. A shelf-life test shows that the improved device performance comes with negligible negative impact of stability: encapsulated devices retain over 90% efficiency after storing in ambient air in that dark at ~30% humidity for 45 d.

In summary, we have demonstrated highly efficient and stable quasi 2D (n = 5) PVSCs by simultaneously incorporating NH_4SCN and NH_4Cl to tune the orientation, improve the crystallinity, and reduce non-radiative recombination of the quasi-2D perovskite films. Our findings not only represent a milestone for quasi-2D PVSC development but also pave the way for related optoelectronic applications, such as stable perovskite light-emitting diodes.

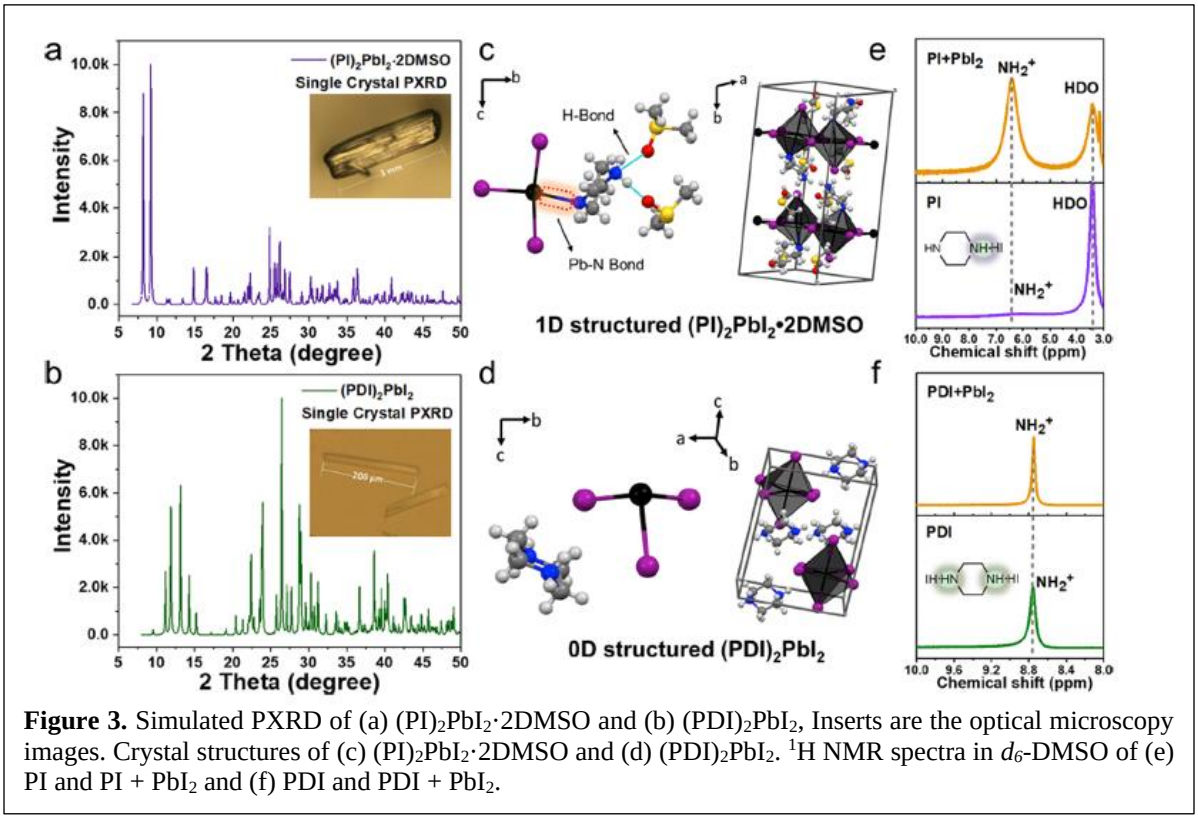

Figure 3. Simulated PXRD of (a) $(PI)_2PbI_2{\cdot}2DMSO$ and (b) $(PDI)_2PbI_2$, Inserts are the optical microscopy images. Crystal structures of (c) $(PI)_2PbI_2{\cdot}2DMSO$ and (d) $(PDI)_2PbI_2$. ^1H NMR spectra in d_6-DMSO of (e) PI and PI + PbI_2 and (f) PDI and PDI + PbI_2.

4.1 <u>Regulating surface termination of 2D hybrid perovskites for perovskite solar cells</u>: Passivating surface and bulk defects of perovskite films has been proven to be an effective way to minimize nonradiative recombination losses in PVSCs in order to further enhance the V_{OC} and PCE. The lattice interference and perturbation of atomic periodicity at the perovskite surfaces (e.g. positive Pb_2^+ traps and negative halide traps) often significantly affect the material properties and device efficiencies. By tailoring the terminal groups on the perovskite surface and modifying the surface chemical environment, the defects can be reduced to enhance the photovoltaic performance and stability of derived PVSCs.

Although numerous molecules have been developed to tailor the surface chemical environments and surface defects, most of them only passivate either the positively or negatively charged defects. There are very few molecules that can passivate both Pb_2^+ and halide ion traps on the perovskite surface. We have rationally designed a bifunctional molecule, piperazinium iodide (PI), containing both R_2NH and $R_2NH_2^+$ groups on a six-membered ring, behaving both as an electron donor and an electron acceptor to react with different surface-terminating ends on perovskite films. The resulting perovskite films with the defect passivation showed release of surface residual stress, suppressed nonradiative recombination loss. It was found that PI could form a Pb−N bond in the single crystal of $(PI)_2{\cdot}PbI_2{\cdot}2DMSO$, which was grown as a model compound to investigate the chemical interactions between PI and PbI_2 (**Figure 3**). After

introducing PI for surface treatment, the residual stress of the film surface could also be released. The tuning of surface termination with PI treatment also helps to achieve a more n-type enriched film characteristics to facilitate charge transfer. The combined effects resulted in a high V_{OC} of 1.17V and a significantly reduced V_{OC} loss of 0.33 V due to the suppressed nonradiative recombination loss. An extremely high power conversion efficiency of 23.37% (with 22.75% certified) could be achieved, which is one of the highest value reported for inverted PVSCs. Our work reveals a very effective way of using rationally designed bifunctional molecules to simultaneously enhance the device performance and stability.

To understand the details of passivation effect of PI, the recombination occurring in the perovskite films was investigated by steady-state Photoluminescence (PL) and Time-Resolved Photoluminescence (TRPL) analysis (**Figure 4a-b**). The PL intensities of perovskite films after PI and PDI treatments were about 5 and 3 times higher than those of the reference films, suggesting that their nonradiative recombination loss is alleviated considerably after surface passivation. Moreover, we found that the perovskite films after PI and PDI surface treatments possessed a longer carrier lifetime compared to that of the reference film. The average lifetime (τ_{avg}) values of the reference perovskite film and PI and PDI treated films are 305, 1948, and 1461 ns, respectively. The significantly prolonged lifetimes of perovskite films after PI and PDI treatments were attributed to the suppressed defects such as lead clusters, undercoordinated halides, and Pb−I anti-site which usually cause nonradiative recombination. The combined effects of R_2NH and $R_2NH_2^+$ groups on PI for defect passivation are superior to those obtained from PDI with only the $R_2NH_2^+$ group, which demonstrates the benefit of having multifunctional passivator.

Confocal PL mappings were also conducted to explore the optoelectronic properties of perovskite films (**Figure 4c-e**). The PL intensity in the central area of a single grain is much higher than those from the grain boundaries, which indicates better charge transfer with minimized recombination. After the PI treatment, overall PL intensity is significantly improved and the intensity distribution was more homogeneous compared to those obtained from the reference and PDI treated films. The distribution of PL peaks on the perovskite film is considerably narrower after PI treatment, suggesting that the surface phase segregation is suppressed.

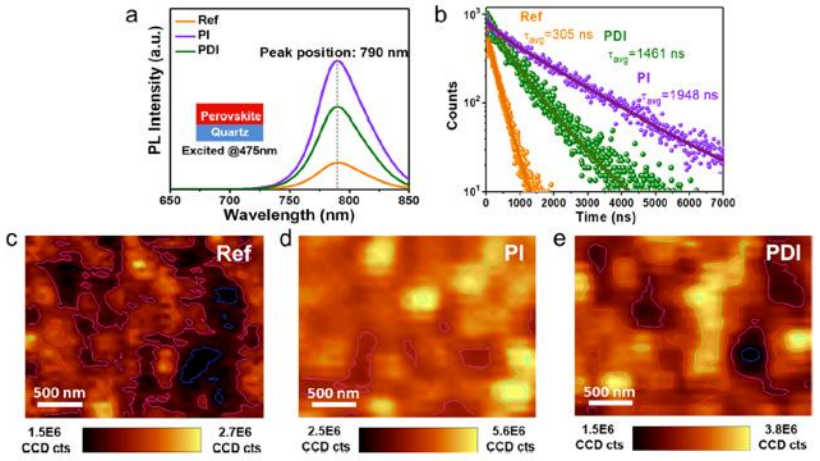

Figure 4. (a) Steady-state PL spectra and (b) time-resolved photoluminescence plots of perovskite films. Confocal PL intensity maps of (c) reference perovskite film and perovskite films with (d) PI and (e) PDI treatments. The

contour in the pictures represents the auto level of PL intensity, with the sequence of blue, purple, magenta, red, green, and cyan.

In summary, we found a rationally designed bifunctional molecule, piperazinium iodide, containing both R_2NH and $R_2NH_2^+$ groups on a same ring passivates surface and bulk defects of perovskite films effectively and minimize nonradiative recombination losses in PVSCs. As a result, a very high PCE of 23.37% was achieved, which is one of the highest value reported for inverted PVSCs.

4.3 <u>Coordination engineering of single-crystal precursor for phase control in Ruddlesden-Popper perovskites</u>: 2D Ruddlesden–Popper Perovskites (RPPs) with a general formula $(A')_2(A)_{n-1}Pb_nI_{3n+1}$ (A′ is a primary monovalent cations) have recently drawn significant attention because of their structural variability that can be used to tailor optoelectronic properties and improve the stability of derived photovoltaic devices. However, charge separation and transport in 2D PVSCs suffer from quantum well barriers formed during the synthesis of perovskites. It is extremely difficult to manage phase purities in 2D perovskites made from the stoichiometric mixtures of precursor solutions. Cationic organic spacers used also lead to a strong quantum and dielectric confinement in 2D perovskite. Moreover, the decreased conductivity of the organic layers hinders the carrier charge transport between perovskite quantum wells. Thus, RPP exhibits a wider bandgap, a higher exciton binding energy (Eb), and lower charge mobility relative to the 3D perovskites, which results in poor efficiencies for device applications. Nonetheless, through rational design of organic spacer cations with more conductive conjugated spacers, interlayer coupling in 2D perovskites could be promoted to enhance charge transport between quantum wells.

RPP films with large n values exhibit features similar to their 3D counterparts and a trade-off between the PCE and stability has to be made in such case. At low dimension ($n \leq 3$), improvement in device efficiency can be achieved by optimizing two key properties of the RPP films: phase distribution and crystal orientation. On one hand, an effective approach to facilitate the vertical orientation of RPPs is depositing the 2D perovskite film by either introducing additives or at elevated temperature. On the other hand, effective control of the phase distribution in RPPs is difficult for conventional solution-fabrication using dissolution of a stoichiometric mixture of the precursor components in polar solvents, such as DMF, DMSO, and DMAc. We have devised coordination engineering of a single crystal derived precursor to provide control over the phase purity and arrangement in high-quality RPP films. Inspired by ligand-assisted reprecipitation methods in colloidal synthesis of perovskite nanocrystals (bottom-up), we dissolved $(TEA)_2(MA)_2Pb_3I_{10}$ (TEA = 2-thiophene ethylamine) single crystals in a mixed DMAc:TOL (HI) solvent as a precursor solution for perovskite films (top-down). The use of HI can decrease the coordinating strength between PbI_2 and DMAc, resulting in slow decomposition of the layered structure that can be further isolated by the poorly-coordinating solvent toluene (TOL) to maintain intrinsic n = 3 units in colloidal solution. We found that highly desired RPP films with narrow phase distribution with preferentially perpendicular crystal orientation result in a remarkable improvement in photovoltaic performance and reproducibility.

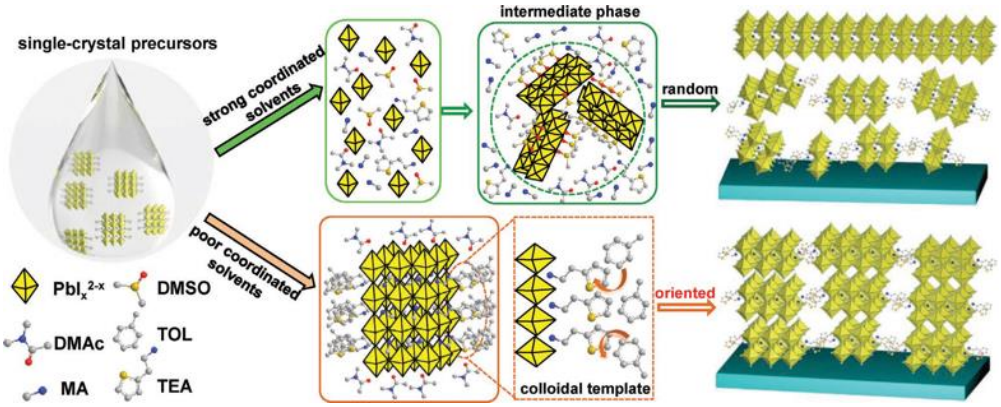

Figure 5. Graphic illustration showing the transformation of colloidal phase into either random or highly oriented RPP films from single-crystal starting material in various solvents.

We propose a model to illustrate the crystallization process from a single crystal precursor as shown in **Figure 5**. $(TEA)_2(MA)_2Pb_3I_{10}$ crystals are dissolved in DMAc first and colloidal phase solution is formed. The colloidal phase can be transformed into either random or highly oriented RPP films by using solvents with different coordination strength. Using a cosolvent with strong coordinating abilities for metal halides, the colloidal phase can be further solubilized by allowing facile intercalation of guest DMSO molecules into the organic spacer then decomposes into individual ions, including TEA^+, MA^+, and $PbI_2(DMSO)_x$ complexes. Similar to the conventional stoichiometric recipe, the nontemplate ions would partially convert into the more thermodynamically favorable low n-number phases and $n = \infty$ phase, rather than self-assemble back into the $n = 3$ perovskite. Using a poorly coordinating cosolvents highly oriented RPP films are resulted due to the self-assembly of colloidal precursors.

In summary, we have demonstrated a generally applicable synthesis method to control phase purity and arrangement in RPP films. By the colloidal formation of of single-crystal precursors in solution, precise coordination engineering was achieved with a rationally selected cosolvents to tune the colloidal properties. In nonpolar cosolvent media, the derived colloidal precursors enables RPP crystals to preferentially grow along the vertically ordered alignment with a narrow phase variation, resulting in efficient charge transport and extraction. As a result, a very high PCE of 14.68% is demonstrated for a $(TEA)_2(MA)_2Pb_3I_{10}$ ($n = 3$) PVSC with negligible hysteresis. Remarkably, superior stability is achieved with 93% of the initial efficiency retained after 500 h of unencapsulated operation in ambient air conditions.

4.4 <u>Mixed metal halide perovskite single crystals with tunable band gaps:</u> The mixed metal Pb/Sn halide perovskites have drawn significant attentions due to their broad absorption spectra and tunable band gaps. To obtain a deeper understanding of these materials properties, single crystals are regarded as the best platform among various building blocks for fundamental study. We have prepared the mixed-metal $MAPb_xSn_{1-x}Br_3$ ($MA = CH_3NH_3$) perovskite single crystals grown by top seeded solution growth (TSSG) method. Systematical characterizations were applied to investigate their structures and optoelectronic properties. These single crystals kept higher stability even exposed to air over one month than that of $MASnBr_3$. The outstanding electrical properties, such as lower trap-state density and higher carrier mobility, were investigated by space charge-limited current (SCLC) and the Hall Effect measurements. More importantly, these perovskite single crystals exhibited much narrower optical band gap (1.77 eV)

and longer carrier lifetime (~2 μs) than those of $MAPbBr_3$ and $MASnBr_3$, which showed a great application potential in tandem photovoltaic devices with the optimal bandgap of 1.70–1.85 eV.

In principle, optical band gap and optoelectronic properties of metal halide perovskites AMX_3 can be tailored by the selection of M^+ and X^- ions, while the variable cations on the A^+ sites play a critical role on its lattice torsion and associated phase transformation. It is worthwhile to note that mixed halide anions (Br/I) compounds with tunable bandgaps often present photoinduced phase segregation caused by halide ion migration. Nevertheless, the researchers have found mixed Pb/Sn, can effectively mitigate the Br/I phase segregation to prepare stable and efficient PVSCs with tunable bandgaps ranging from 1.17 to 1.73 eV with a M-site alloy. However, the progress of Pb/Sn based PVSCs has been still hindered by the chemical instability of Sn^{2+} element. To further explore the fundamental properties of these materials, large-size high quality hybrid perovskite single crystals can be served as an ideal scaffold due to the fewer grain boundaries and surface defects. Better understandings of their structure, optoelectronic properties and stability enabled us to optimize their derived photoelectric devices. Recently, growth of mixed organic cations A^+ or halide anions X^- single crystals has also been reported. However, there have been few reports pertaining to mixed Pb/Sn hybrid perovskite single crystals due to the oxidation of Sn^{2+} to Sn^{4+} easily.

We have grown mixed $MAPb_xSn_{1-x}Br_3$ single crystals with large macroscopic dimensions (16 × 14 × 10 mm) using TSSG method in ambient atmosphere. We have systematically characterized the mixed crystal system using powder and single crystal X-ray diffraction, UV–vis spectra, and thermogravimetric analysis, etc., were used to elucidate the intrinsic structure and optoelectronic properties of the synthesized single crystals in detail. Interestingly, mixed $MAPb_xSn_{1-x}Br_3$ single crystals exhibited high stability when exposed to air. More importantly, mixed $MAPb_xSn_{1-x}Br_3$ single crystals demonstrated much narrower optical band gap and longer carrier lifetime. These behaviors revealed the intrinsic optical and electric properties of the mixed Pb/Sn hybrid perovskite materials, which provide a guidance for future application of their optoelectronic devices.

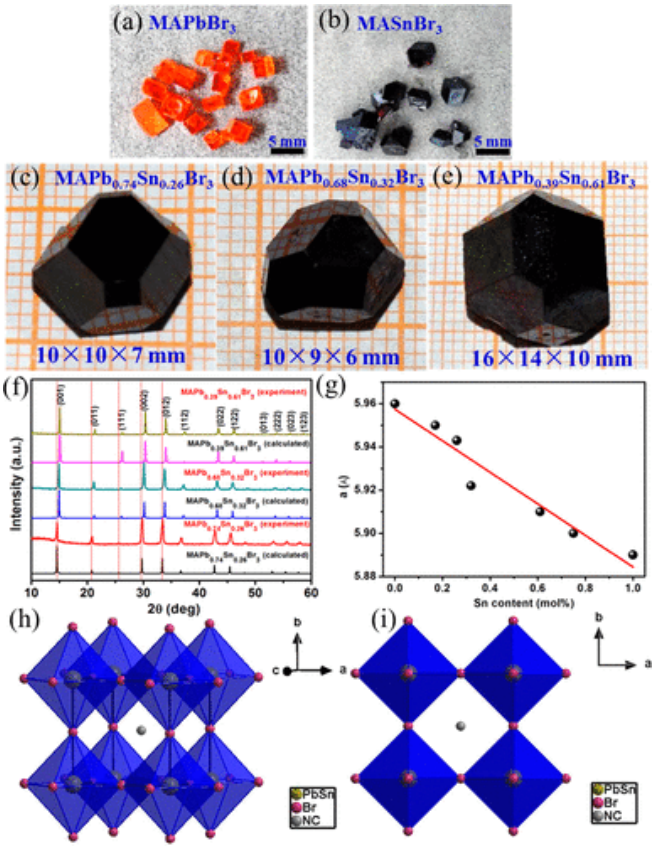

Figure 6. $MAPb_xSn_{1-x}Br_3$ single crystals obtained by tuning the Pb/Sn molar ratios. (a)$MAPbBr_3$, (b) $MASnBr_3$, (c) $MAPb_{0.74}Sn_{0.26}Br_3$, (d) $MAPb_{0.68}Sn_{0.32}Br_3$, (e) $MAPb_{0.39}Sn_{0.61}Br_3$. (f) Experimental and calculated powder X-ray diffraction patterns for kinds of $MAPb_xSn_{1-x}Br_3$ powder. The powder XRD patterns of the samples were consistent with the calculated XRD patterns of these single crystals. (g) The variation in cubic lattice parameters with a change in Sn contents. (h–i) Ball-and-stick diagrams of crystal structures and their ($(Pb/Sn)Br_6$) octahedral structure units in the $MAPb_xSn_{1-x}Br_3$ single crystals. The C and N elements represent the disordered CH_3NH_3 groups; hydrogen atoms bonded to the C or N atoms were

omitted for clarity.

Figure 6a-e show bulk $MAPb_xSn_{1-x}Br_3$ single crystals with a black, reflective surfaces. Compared with the $MAPbBr_3$ (**Figure 6a**) and $MASnBr_3$ (**Figure 6b**), the color of mixed perovskite $MAPb_xSn_{1-x}Br_3$ single crystals (**Figure 6c-e**) darker clearly. This can also be observed from their powder and micrometer size single crystals, which the color of $MAPb_xSn_{1-x}Br_3$ microcrystals darkening with the increase of concentration of Sn^{2+} ions. Powder X-ray diffraction patterns of these crystals confirmed the pure perovskite phase of $MAPb_xSn_{1-x}Br_3$ single crystals. XRD diffraction patterns match well with the calculated XRD patterns, as shown in (**Figure 6f**). With the increasing concentration of Sn^{2+}, a small shift in the XRD peaks toward the larger angle was exhibited, which suggests the decrease of lattice parameters due to the smaller ionic radius of Sn^{2+} than that of Pb^{2+}. This agrees well with the variation of cubic lattice parameters for $MAPb_xSn_{1-x}Br_3$ in (**Figure 6g**). With the molar ratio of Pb and Sn of 3:1 and1:4, we prepared two additional single crystals with their lattice parameters and compositions determined by the single crystal X-ray diffraction. The crystal structures indicate that all the $MAPb_xSn_{1-x}Br_3$ crystals belong to the cubic perovskite phase in *Pm-3m* space group at room temperature, which are the same with $MAPbBr_3$ and $MASnBr_3$.

The air stability is an important factor for the application of hybrid perovskite. $MAPb_xSn_{1-x}Br_3$ single crystals we have grown exhibited good air stability even after exposure to the atmosphere for one month, which was confirmed by XRD and XPS. More importantly, the oxidation state of Sn remains unchanged before and after one month of air exposure, demonstrating good ambient stability of the $MAPb_xSn_{1-x}Br_3$single crystals. Moreover, the $MAPb_{0.39}Sn_{0.61}Br_3$ single crystals also kept their relative stability even after exposure to high humidity atmosphere (70 RH%) for 24 hours.

In summary, we have successfully obtained a series of centimeter-size $MAPb_xSn_{1-x}Br_3$ single crystals and demonstrated their structural and optoelectronic properties by XRD, UV–vis, thermogravimetric analysis, space charge-limited current and the Hall Effect measurements, etc. By carefully regulating the Sn^{2+} content, the optical band gaps of $MAPb_xSn_{1-x}Br_3$ single crystals were greatly decreased and the carrier lifetime was greatly delayed compared with that of those $MAPbBr_3$, which is useful for photovoltaic applications, especially for tandem solar cells. Moreover, mixed Pb/Sn single crystals demonstrated improved stability than $MASnBr_3$ in the ambient atmosphere over one month. Our investigations of Pb/Sn single crystals revealed the role of mixed-metal cations in hybrid perovskite materials with a lower band gap to facilitate the design of highly stable mixed-metal hybrid perovskite for optoelectronic device applications.

4.5 Ion exchange procedures between multidimensional hybrid perovskites: Although the direct solution growth provides a more convenient way for mono- and bi-layer perovskite growth, their experimental conditions including temperature, selected solvents, and concentrations still need to be carefully engineered in order to achieve different material systems. To alleviate this tedious process, we have developed simple reversible ion exchange procedures between multidimensional hybrid perovskites as a simple and generally applicable method for to synthesize diverse classes of 2D hybrid perovskites (**Figure 7**).

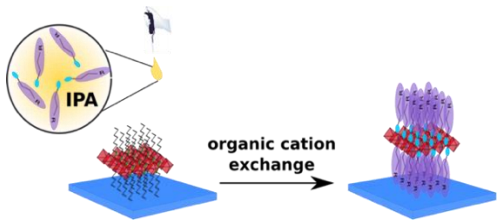

Figure 7. Schematic illustration of ion exchange procedure for universal 2D hybrid perovskite growth method.

Since organic and inorganic components have different solubilities, the organic ammonium salt can be dissolved in alcohols (methanol, ethanol or isopropanol) without affecting the metal halides. Therefore, we can simply exchange the organic cations in as-grown perovskite sheets by adding the isopropanol solution of different organic ammonium salt onto the as-grown perovskite crystals of interest. The ion exchange can proceed based on the Le Chatelier's principle until completion. Our experience of growing high quality mono- and bilayer $(C_4H_8NH_3)_2PbBr_4$ allowed us to prepare similar quality of atomically thin 2D hybrid perovskites with desirable organic cations through the ion exchange method. We have developed an ion exchange method for conversion from 2D to 3D perovskites and grow highly oriented $MAPbBr_3$ thin films. We found that the transition between 2D and 3D perovskites by ion exchange is not reversible for all 2D perovskites. The thermodynamics of this exchanges can be affected by intermolecular interaction of anchoring ammonium groups of 2D perovskite organic cations. A monoamine-based 2D perovskite PEA_2PbBr_4 was selected as a model compound and successfully exchanged into $MAPbBr_3$. The resulting $MAPbBr_3$ thin films show improved substrate coverage and with highly aligned orientation of the original 2D perovskite preserved. Improved film characteristics lead to extremely narrow green EL with a record 15.3 nm (67 meV) FWHM compared to ~20 nm reported so far as narrowest and possessed 98.10% color purity. This demonstrates the potential of ion exchange in conjunction with a 2D perovskite growth template as a new processing method to fabricate high-quality perovskite thin films for optoelectronic applications.

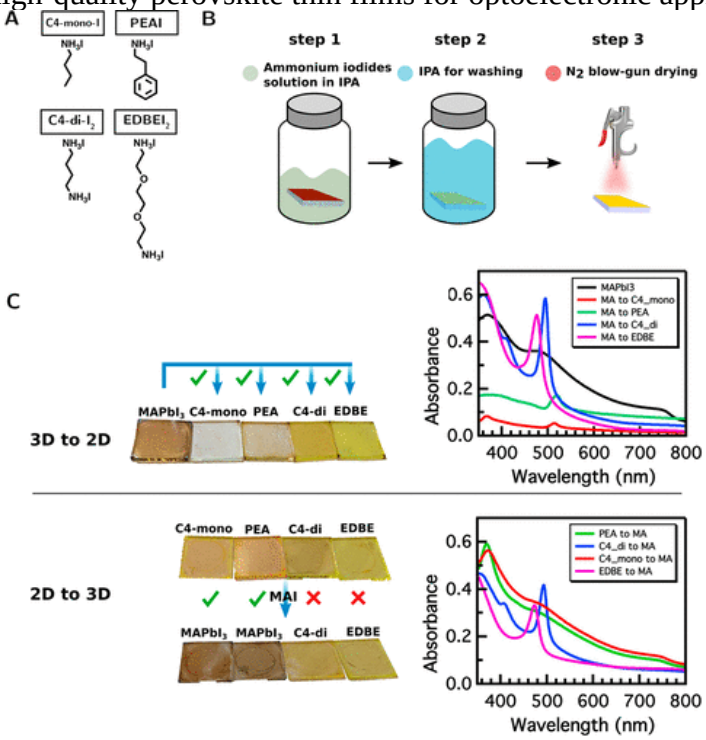

Figure 8. (a) Molecular structure of four ammonium iodides: C4-mono-I, PEAI, C4-di-I_2, and $EDBEI_2$. (b) Schematic illustration of the ion exchange process in this study. (c) Color change and UV–vis absorption feature evolution of thin films before and after ion exchange. The top and bottom correspond to 3D to 2D conversion and 2D to 3D conversion, respectively.

Four different ammonium iodides, which all form 2D perovskites when mixed with lead iodide, were selected to study the ion exchange reaction mechanism between the corresponding 2D perovskites and $MAPbI_3$. They are $CH_3(CH_2)_3NH_3I$ (C4-mono-I), $C_6H_5(CH_2)_2NH_3I$ (PEAI),

$NH_3I(CH_2)_4NH_3I$ (C4-di-I_2), and $NH_3I(CH_2)_2O(CH_2)_2O(CH_2)_2NH_3I$ ($EDBEI_2$); their molecular structures are shown in **Figure 8**. All four 2D perovskite thin films were dipped in MAI solution in isopropanol to test if the 2D perovskites can be converted into $MAPbI_3$ (**Figure 8b**). Similarly, the reverse reaction was initiated by dipping $MAPbI_3$ thin films into C4-mono-I, PEAI, C4-di-I_2, and $EDBEI_2$ solutions in isopropanol, respectively. Going from 3D to 2D, after ion exchange, the film color changed from brown to yellow, with the appearance of exciton absorption peaks at 490–520 nm and the disappearance of $MAPbI_3$ band-edge absorption at 780 nm (**Figure 8c**). Both indicate successful conversion from 3D $MAPbI_3$ to 2D perovskites. Surprisingly, under these conditions, the conversion from 2D to 3D perovskite does not occur to all four materials, as observed in the bottom part of **Figure 8c**. The failed transition from (C4-di)PbI_4 and (EDBE)PbI_4 to $MAPbI_3$ indicates a significant difference between monoamine- and diamine-based 2D perovskites with regard to this ion exchange process.

In addition to the difference in film coverage between reference and exchanged $MAPbBr_3$ films, a large improvement in crystallinity and orientation order was found in the exchanged film. The 2D XRD patterns of the three films are shown in **Figure 9**. In 2D XRD, the γ degree is defined as the direction of the diffracted beam on the diffraction cone, so that the distribution of γ of a specific 2θ diffraction represents the orientation order of the related plane in the crystal. Comparing the (100) diffraction from the reference and the exchanged $MAPbBr_3$, the former shows a ring spanning over the whole detector area and the intensity at different γ degree is similar (**Figure 9a**). Strikingly, the latter shows very confined diffraction signals concentrated at the middle region of the detector. This indicates that the reference film is polycrystalline with random crystallite orientation, while the exchanged film is highly oriented with the (100) plane mostly parallel to the substrate. The preferred [100] growth in the exchanged film can also be evidenced by weakening of the (110) diffraction. To quantitatively analyze the orientation order, a γ scan was conducted on reference and exchanged films for (100) diffraction.

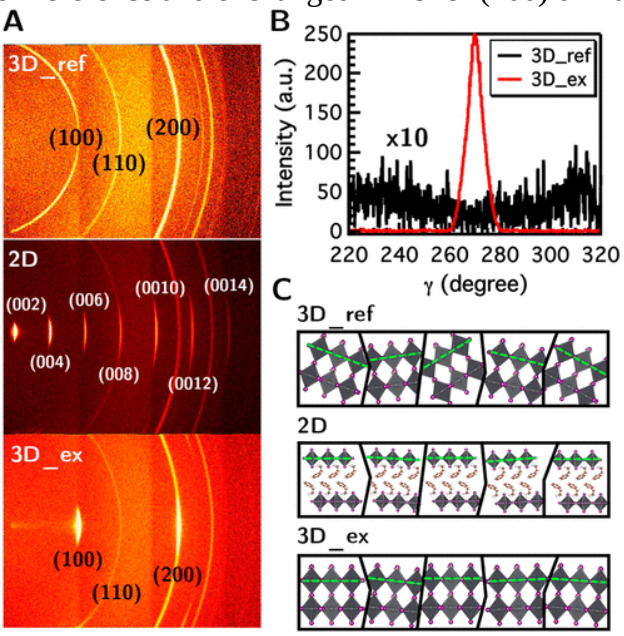

Figure 9. (a) 2D XRD pattern and (c) schematic illustrationn of the crystallite orientation in 3D_ref, 2D, and 3D_ex. (b) XRD intensity versus gamma of 3D_ref and 3D_ex thin films (magnified 10 times for the 3D_ref film due to its weak XRD intensity). Note: "3D_ref", "3D_ex", and "2D" correspond to reference $MAPbBr_3$, exchanged $MAPbBr_3$, and PEA_2PbBr_4 films, respectively.

As shown in **Figure 9b**, the reference film shows no observable feature, confirming its random crystallite orientation, while the exchanged film shows a distinct peak with a FWHM of 7.06°. This much-improved orientation order after ion exchange can be attributed to templates provided by 2D perovskites, which preferably induce the growth in the [001] direction. Suggested crystallite orientations are schematically illustrated in **Figure 9c**. To test the generality of ion exchange from 2D to 3D perovskite for controlling the orientation of perovskite thin films, we have performed the same 2D XRD characterization on iodide-based perovskites. Strong texture can be observed in the resulting $MAPbI_3$ film exchanged from PEA_2PbI_4, similar to the bromide-based perovskites discussed. This result demonstrates the effectiveness of this method in tuning grain orientation independent of the halide composition.

Besides higher orientational order, the excess amount of MABr in solution during ion exchange can potentially reduce the equilibrium concentration of vacancy defects (V_{MA} and V_{Br}), which are otherwise readily formed in large quantity because of their lower formation energies. We therefore performed PL studies to assess the optoelectronic quality of the exchanged film in comparison to reference $MAPbBr_3$. As observed from the PL spectra, the exchanged film has ~10 times higher PL intensity compared to reference film. The dramatic increase in PL intensity implies enhanced radiative recombination and is indicative of the improved quality of the exchanged film. To further assess the optoelectronic quality of the exchange film, we measured time-resolved PL and observed a 33% average lifetime increase in the exchanged film compared to the reference, which indicates reduction of trap states. Thus, the increased PL intensity, PL blue shift, and higher average lifetime altogether confirm the higher quality of the exchanged film with reduced non-radiative recombination centers compared to the reference film. The higher orientational order and improved optoelectronic quality achieved using the ion exchange technique is promising, and the exchanged $MAPbBr_3$ has great prospects for high color purity light emission applications (**Figure 10**).

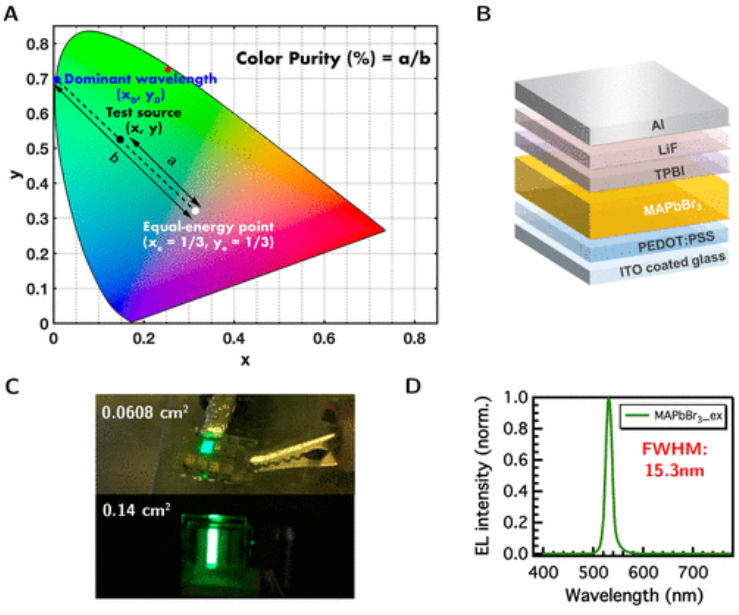

Figure 10. (a) Color coordinates of the fabricated device and definition of color purity on the CIE 1931 color space. The color purity or color saturation of a light source is the distance in the chromaticity diagram between the (*x*, *y*) color coordinate point of the test source and the coordinate of the equal-energy point (*x*e = 1/3, *y*e = 1/3) divided by the distance between the equal-energy point and the dominant-wavelength point (*x*D, *y*D). (b) Device architecture, (c) green light emission photos, and (d) EL spectrum of MAPbBr3 LEDs using the ion exchange processing method.

In summary, we have discovered selective ion exchange reactivity between 2D and 3D perovskites. We have found that the intermolecular interaction and ammonium functionality of organic cations largely affect the thermodynamics and kinetics of this ion exchange reaction. Conversion from 2D to 3D perovskites can be inhibited thermodynamically when strong hydrogen bonding exists between adjacent organic cations, which stabilizes the

structure. Diammonium functionality can induce a more robust crystal lattices, which raises the energy barrier for the ion exchange reaction and thus prevents the 2D to 3D conversion. With a better understanding of the reaction conditions and mechanism, we successfully exchanged a PEA_2PbBr_4 thin film into $MAPbBr_3$. The resulting film has an improved morphology and better coverage. Benefiting from the preferred growth of PEA_2PbBr_4 in the [001] direction, the $MAPbBr_3$ after exchange exhibits high orientational order. This improved order is associated with a reduce crystallographic defect density, and the resulting films exhibit extremely narrow green light emission with a FWHM as narrow as 15.3 nm and color purity as high as 98.10%.

4.6 <u>Tailoring the functionality of organic spacer cations for efficient and stable 2D hybrid perovskites</u>: Recent development of quasi-2D PVSCs have drawn significant attention due to the improved stability of these materials and devices fabricated based on them against moisture compared to their 3D counterparts. However, the optoelectronic properties of 2D perovskites need to be optimized further to achieve high efficiency. We have systematically studied the effect of spacer cations, i.e., phenethylammonium (PEA), 4-fluorophenethylammonium (F-PEA) and 4-methoxyphenethylammonium (MeO-PEA) on the optoelectronic properties and device performance of quasi-2D perovskites. We found that both larger and more hydrophobic cations can improve perovskite stability against moisture, while larger size can adversely influence the device performance. Interestingly, with F-PEA or MeO-PEA, distribution of n value can be shifted toward high 3D content in quasi-2D perovskite layer, which enables lower bandgaps and possibly lower exciton binding energy. Due to the better charge transport and lowest bandgap, F-PEAI-based qusai-2D perovskite (n = 5) among the series solar cell shows a highest PCE of 14.5% with excellent stability in air with a humidity of 40-50%, keeping 90% of the original PCE after 40 days. We believe this approach open a way for the design of new organic spacer cations for stable quasi-2D hybrid perovskites with improved performance.

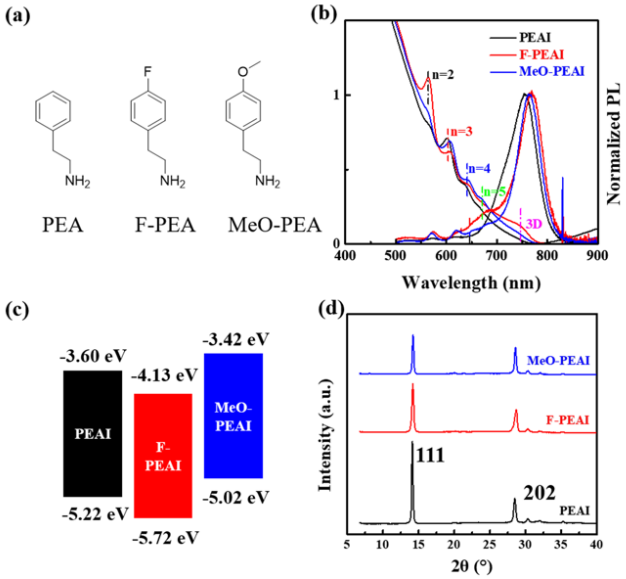

Figure 11. (a) Molecular structures of the organic spacer ligands used in this work, PEA, F-PEA, MeO-PEA. Absorption and photoluminescence spectra, (b) energy level diagram (c) and XRD patterns (d) of quasi-2D perovskites with various organic spacer ligands.

We have designed and synthesized a series of phenethylammonium (PEA) derivatives with fluorine substituent at the para position (4-fluorophenethylammonium, F-PEA) or larger size methoxy group (4-methoxyphenethylammonium, MeO-PEA) as organic spacer cations to study their influence on the optoelectronic properties and stability for 2D perovskites. Notably, the F-PEAI-based quasi-2D (n = 5) PVSC shows excellent stability in air (with 40-50% humidity), keeping 90% of the original PCE after 40 days with PCE of 14.5% as a result of improved charge-transporting properties and small bandgap. The molecular structures of the organic spacer PEA, F-PEA, MeO-PEA for quasi-2D perovskite (n =5) are shown in **Figure 11a**. NH_4SCN and NH_4Cl were used as additives to achieve highly crystalline and vertically aligned quasi-2D perovskites as reported in our previous work. The formation of vertical alignment is critical for charge transport to achieve high performance. Compact and uniform films were formed with various cations as shown by Scanning Electron Microscopy (SEM). Optical properties of the the quasi-2D perovskites (n =5) thin films were investigated by UV-Vis and PL spectra shown in **Figure 11b**. The optical bandgaps decrease slightly when the organic spacer amines changes from PEA (1.61 eV) to F-PEA (1.60 eV), and MeO-PEA (1.59 eV). F-PEAI-based quasi-2D perovskite shows the smallest bandgap of 1.59 eV due to the formation of high n value perovskites, similar with the ALA-based quasi-2D perovskite. The PL spectra also indicate that the F-PEAI and MeO-PEAI-based quasi-2D perovskites contain high n value perovskites and a narrower n distribution. These results suggest that organic spacer ligands affect the quantum well width and distribution. The energy levels were measured by Ultraviolet Photoelectron Spectroscopy (UPS), the corresponding energy level diagrams were shown in **Figure 11c**. Due to the different molecular dipoles of organic spacer cations, the energy level varies. The F-PEAI-based quasi-2D perovskite shows deeper valance band (VB) and conduction band (CB), while the MeO-PEAI-based quasi-2D perovskite shows higher VB and CB relative to PEAI based one.

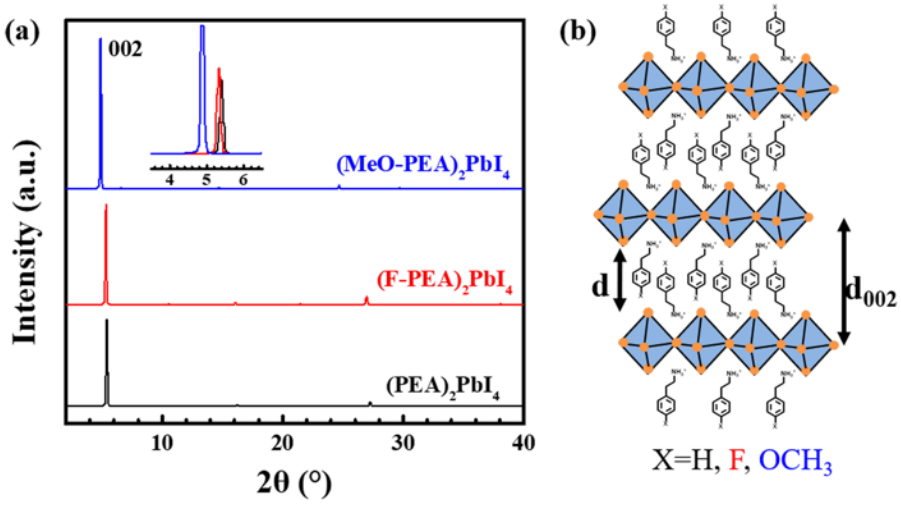

Figure 12. (a) XRD patterns of 2D perovskite (n=1) with various organic spacer ligands. (b) Schematic illustration of the 2D perovskite.

The crystallinity of the quasi-2D perovskites were investigated by XRD (**Figure 11d**). The XRD patterns show two dominant diffraction peaks at 14.14° and 28.50°, but lack (0k0) reflections, indicating good crystallinity and vertical growth of the quasi-2D perovskite films. The intensity of peak at 14.14° decreases when the organic spacer amines was changed from

PEAI to F-PEAI or MeO-PEAI. The MeO-PEAI-based quasi-2D perovskite film shows the lowest crystallinity possibly due to the larger size. The size of the organic cation also affects the interlayer distance of the quasi-2D perovskite (**Figure 12**). The (002) peaks show different peak positions for 2D perovskite (n = 1) with varying cations, and this is related to the interlayer distance between 2D perovskite layers. The interlayer distances are 10.10, 10.33 and 11.79 Å for PEAI, F-PEAI and MeO-PEAI-based 2D perovskites, respectively. Quasi-2D perovskites with shorter interlayer distance have been demonstrated to show higher photovoltaic performance.

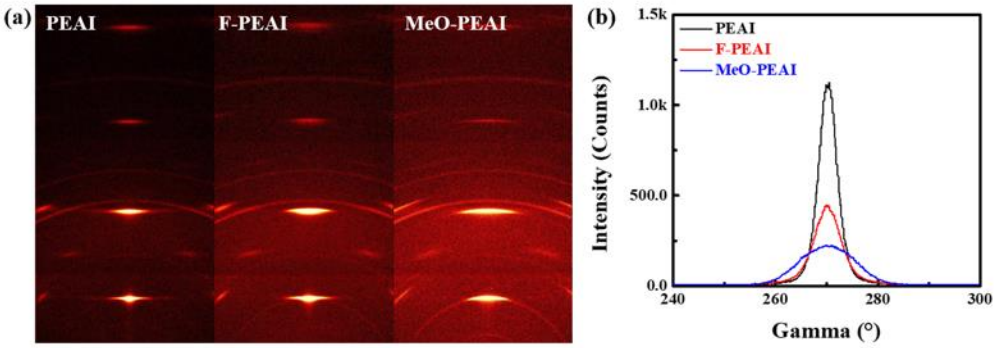

Figure 13. (a) 2D-XRD images of 2D perovskite films with different organic ligands. (b) Gamma vs intensity plots at the peak of 14.14°.

Crystallographic measurements using 2D-XRD were conducted to probe the perovskite orientation which is critical for charge transport and device performance (**Figure 13a**). The diffraction intensity is highly concentrated in spots, indicating a high degree of preferential crystallographic orientation. The extent of preferential orientation can be further characterized by gamma vs intensity plots (**Figure 13b**). The FWHM increases from 4.2° to 6.0° and 12.6°, respectively when changing PEAI to F-PEAI and MeO-PEAI, while the peak intensity also decreases. Broadening of peak width coupled with a decrease in peak intensity indicating a weaker preferential orientation with a larger organic spacer ligand. Further insight into charge-transporting properties was gained by analyzing electron and hole mobilities of these quasi-2D perovskites with the commonly used Space-Charge-Limited Current measurement. F-PEAI-based quasi-2D perovskite shows the highest electron and hole mobilities of $(8.0 \pm 3.1) \times 10^{-3}$ $cm^2\ V^{-1}\ s^{-1}$ and $(5.2 \pm 2.0) \times 10^{-3}\ cm^2\ V^{-1}\ s^{-1}$, respectively. MeO-PEAI-based quasi-2D perovskite shows a higher hole mobility of $(3.5 \pm 1.0) \times 10^{-3}\ cm^2\ V^{-1}\ s^{-1}$ and a similar electron mobility of $(5.8 \pm 1.9) \times 10^{-3}\ cm^2\ V^{-1}\ s^{-1}$ compared to the hole mobility of $(1.8 \pm 0.5) \times 10^{-3}\ cm^2\ V^{-1}\ s^{-1}$ and electron mobility of $(6.6 \pm 1.9) \times 10^{-3}\ cm^2\ V^{-1}\ s^{-1}$ of PEAI-based quasi-2D perovskite. The improved mobilities might be due to the formation of higher n value perovskites supported by UV-Vis and PL spectra, suggesting efficient charge transport in films.

Air stability of the quasi-2D perovskite films were tested by tracking the absorption spectra and XRD patterns. The samples were stored in air with a humidity of 40-50% at room temperature. The absorption of PEAI-based quais-2D perovskite enhanced after 7 days, then decrease gradually, while the absorption of F-PEAI and MeO-PEAI-based quasi-2D perovskites remain almost the same. XRD pattern of PEAI-based quasi-2D perovskite showed the PbI_2 peak at 12.8° after 28 days, while it took 42 days for F-PEAI-based quasi-2D perovskite to show the same peak. Surprisingly, no apparent PbI_2 peak could be observed for the MeO-PEAI-based quasi-2D perovskite even after 42 days. These results indicate that F-PEAI and MeO-PEAI-

based quasi-2D perovskites possess better ambient stability than PEAI-based quasi-2D perovskite. The vertically orientated highly crystalline quasi-2D perovskite films with significantly improved air stability will help the derived solar cells for potential commercial applications. Planar-structured PVSCs with the device structure of ITO/PEDOT: PSS/(x-PEA)$_2$(MA)$_4$Pb$_5$I$_{16}$/PC$_{61}$BM/BCP/Ag were fabricated to investigate their photovoltaic performance.

In summary, the effects of organic spacer cations, PEA, F-PEA and MeO-PEA, on the optoelectronic properties and stabilities of quais-2D perovskites were studied. MeO-PEAI and F-PEAI-based perovskites show much better stability than PEAI-based perovskite due to the steric effect and hydrophobicity preventing the water from penetrating the perovskite structures. Due to the best charge transport and lowest bandgap among the series, F-PEAI-based qusai-2D perovskite (n = 5) solar cell shows the best PCE of 14.5%. It also shows excellent stability in air keeping 90% of the original PCE after 40 days under a humidity of 40-50%.

4.7 Incorporating delocalized aromatic biimidazolium dication for efficient and stable 2D hybrid perovskites: As described, the structure of 2D perovskites can be systematically tuned by adjusting the composition of perovskite layers and molecular design of the organic spacer cations. Thus, much wider range of optoelectronic properties can be achieved in 2D perovskites than in 3D perovskites. Organic spacer cations with aromatic moieties such as naphthalene, pyrene, or perylene have been demonstrated to enhance the out-of-plane conductivity and photovoltaic performance. In this project, we have introduced insulating alkyl-linker-free, fully aromatic delocalized biimidazolium (BIDZ) dication into the quasi-2D perovskites. The resulting perovskites show enhanced hole and electron mobilities and subsequently improved performance compared to the well-known organic cation PEAI-based quasi-2D perovskites.

As discussed, due to the combination of simple and low-cost solution processing, PVSCs have the potential to compete with current commercially available photovoltaic technologies. However, their inherent instability over moisture, light, and heat remain crucial concerns before it can be considered for commercialization. In this regard, 2D hybrid perovskites have received increasing attention owing to their superior ambient stability due to the bulkier and hydrophobic organic molecules in the material structure. In order to further improve the efficiency of quasi-2D PVSCs there are still several hurdles that need to be overcome, especially for improving the charge transport between the inorganic layers hindered by the insulating bulky organic cations. Increasing highly conductive inorganic layer thickness between two adjacent organic spacers by adjusting the stoichiometric ratios between small and large cations is an effective way to enhance the performance of quasi-2D PVSCs, but this approach sacrifice stability of such structures to certain extent. As discussed earlier, tuning the crystal growth orientation perpendicular to the substrate is one way to mitigate the negative impact caused by insulating bulky groups on out-of-plane conductivity between inorganic layers. Unfortunately, methods to control orientation of 2D hybrid perovskite structures by additives or hot-casting techniques are still not well developed and generally applicable in quasi-2D perovskites based on different organic cations.

The out-of-plane conductivity in n = 1 layered perovskites has been shown to increase several orders of magnitude by using aromatic cations. Thus, designing and incorporating less insulating organic spacers into quasi-2D perovskites is a potentially effective approach to improve both device performance and stability at the same time. Recently, benzimidazolium and benzodiimidazolium cations were incorporated in n=1 2D perovskites demonstrating PCE of

2.3%. We have introduced a conjugated aromatic 2,2-biimidazolium (BIDZ) dication into the 2D hybrid perovskite to study the structures, optoelectronic properties, and device performance. The BIDZ dication, which can act as a two-electron acceptor, is fully conjugated and the pi-electrons are delocalized over the entire molecule. This is in contrast to previously reported organic-inorganic layered perovskites that are formed with primary amines having saturated and unsaturated side chains. Compared to the well-known organic cation PEAI-based quasi-2D perovskite (n=5), BIDZ iodide (BIDZI)-based perovskite shows both enhanced carrier mobility and device performance even without controlling perovskite crystal growth orientation, and possesses a comparable ambient stability of PEAI-based devices.

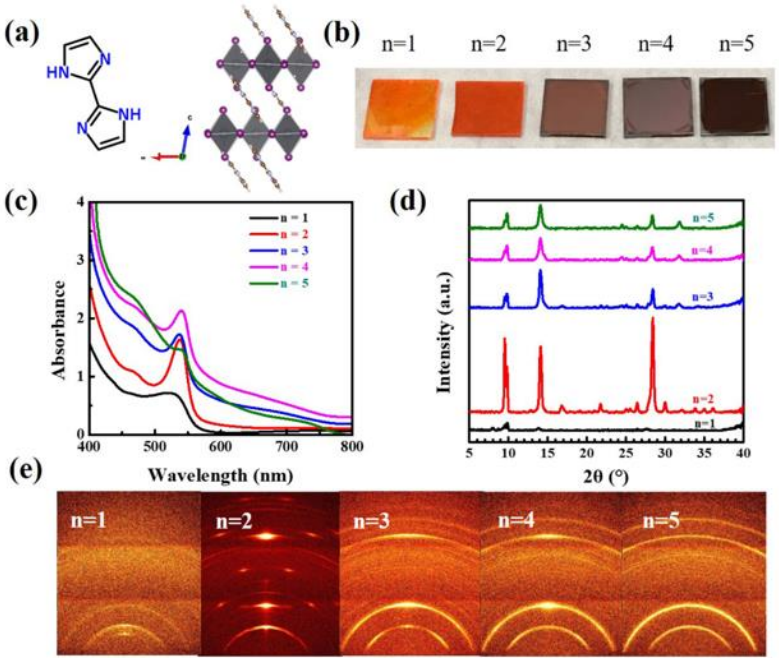

Figure 14. (a) Molecular structure of BIDZ and crystal structure of BIDZPbI$_4$. (b) Optical images, (c) UV-Vis spectra, (d) XRD patterns, and (e) 2D-XRD images of perovskite films processed with ratios of BIDZ: (n-1) MAI: n PbI_2 ratios in DMF.

Figure 14 shows the molecular structure of BIDZ and crystal structure of BIDZPbI$_4$. Quasi-2D perovskite films with a nominal n were processed from precursors with different molar ratios of BIDZI (n = 1 - 5): (n-1) methylammonium iodide (MAI): n PbI_2 in dimethylformamide (DMF) to investigate the film properties. Optical images of resulting 2D perovskite films are shown in **Figure 14b**. We found that the crystallization of n = 1 film is very slow. The color conversion of thin film takes few minutes after spin-coating and annealing at 100 °C on hot plate. This may be due to bulkier biimidazole molecular structure with rigid diammonium functionality leading to slower crystallization rate. The incorporation of MAI accelerates the crystallization process resulting in color change rate comparable to other large cations. **Figure 14c** shows the UV-Vis spectra of the quais-2D perovskites. The absorption spectra of all five films are dominated by the features originated from 3D $MAPbI_3$ with an additional peak located at 540 nm. The latter peak can be attributed to the excitonic absorption of phase pure BIDZPbI$_4$, while no other exciton absorption peaks appear. This is different from other known organic cation-based quais-2D perovskites, which often show a series of exciton absorption peaks (n = 2, 3, 4). Thus, we can infer that the BIDZI-based quasi-2D perovskites prefer to form a mixture of 2D (n = 1) and higher n (at least >5) number quasi-2D hybrid structure. XRD patterns shown in **Figure 14d**

also support the reasoning, which only show one small angle peak at 9.5° (n = 1) throughout all films. **Figure 14e** shows the 2D-XRD images of the perovskite films with various n. We found the orientation of quasi-2D perovskite is highest at n = 2 and it decreases when n increases. For quasi-2D perovskite with n = 5, the crystals are in a random orientation. Unlike the PEAI-based quasi-2D perovskite, we do not effectively tune the orientation of BIDZI-based quasi-2D perovskite for vertical growth relative to substrates by adding additives such as NH_4Cl and NH_4SCN. This is probably due to the structural rigidity of diammonium-based quasi-2D perovskites.

In summary, completely aromatic BIDZ dication with delocalized conjugation pathway connecting highly conductive inorganic layer was introduced into the quasi-2D perovskites. Significantly enhanced hole and electron mobilities were measured in the system and subsequently shown to improve device performance compared to those based on PEAI-based quasi-2D perovskites in random orientation. A highest PCE of 11.4% was achieved with a random perovskite crystal growth orientation. Moreover, the device shows comparable ambient stability with that obtained from PEAI. This may lead to a way for the design of new organic spacer cations for highly efficient and stable quasi-2D perovskites solar cells.

4.8 <u>Development of organic cations for 2D hybrid perovskites based on N-methyl ammoniums as a new anchor group</u>: 2D perovskites are crystalline compounds assembled into a multilayer structure where layers comprising the coordinated metal ions alternate with layers comprising the large cations. The terminal ammonium group of the organic cation interacts with the halides of the inorganic anion layer via both coulombic and hydrogen bonding interactions, and the other parts of molecular structures of adjacent organic cation interact through van der Waals forces to form organic layers. The organic cations incorporated can greatly influence the electronic properties of the inorganic layer by twisting the inorganic framework. The tolerance of layered perovskite materials toward such structural modifications of the organic cations offers new opportunities for tuning the perovskite material properties. Despite the potential for 2D perovskites and the advantages they present over their 3D counterparts, current 2D perovskites still have limitations in design flexibility, economical synthesis, and semiconducting and switching property functionalities. Therefore, there remains a needs for improved perovskite materials which alleviate these problems and to expand the diversity of 2D perovskites even further and explore their influence on the desirable properties in optoelectronic devices.

Organic cation in a 2D hybrid perovskite does not contribute to band structure directly in general, and acts only to neutralize charge within the lattice. However, its size and shape are important. Size of organic cation can cause the whole lattice to expand or contract. Changing the metal halide bond length has been known to affect band structure significantly. The extent of the in- and out-of-plane angular distortions, twisting and buckling of the anionic planes, is largely determined by the relative charge density, steric requirements, and hydrogen-bonding pattern of the organic cations. These distortions correlate with the band structures of the perovskite-type semiconductors. Thus, much wider range of optoelectronic properties can be achieved in 2D perovskites than in 3D perovskites, conferring them the opportunity for broader range of applications. In most reported 2D hybrid perovskites, the organic cations are terminated with primary ammonium groups, and protons on the ammonium form hydrogen bonds to the bridging and terminal halogen atoms in the inorganic layers. Among them, PEA and BA have been, by

far, the most used cations. Most of known cations are based on primary ammoniums as an anchor group interacting with the anionic cavities of metal halide layers. Some of the best reported perovskite solar cells use cations such as PEA to prepare the 2D/3D mixed perovskite materials.

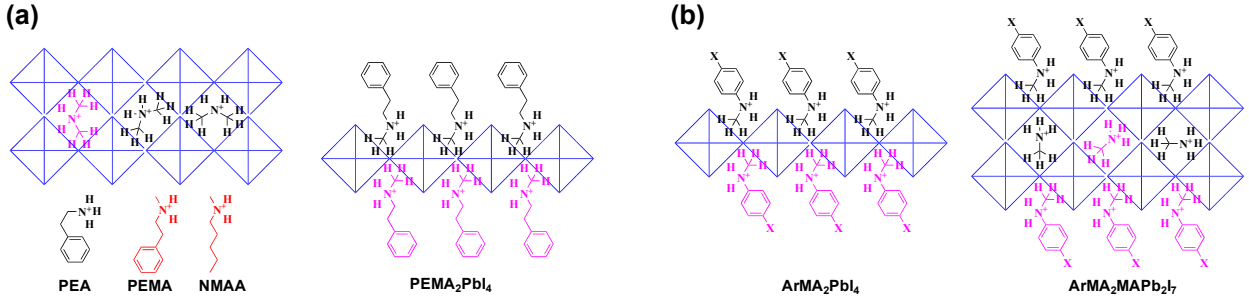

Figure 15. (a) Graphic illustration of molecular structures of 2D hybrid perovskites based on N-methyl ammonium terminal anchor group compared to traditional primary ammonium groups. The anchor group interact with inorganic layers via electrostatic and hydrogen bonding interactionsat the anionic cavities, (b) illustration of proposed molecular structures of 2D hybrid perovskites with N-methyl aryl ammonium anchor group for n=1 and n = 2.

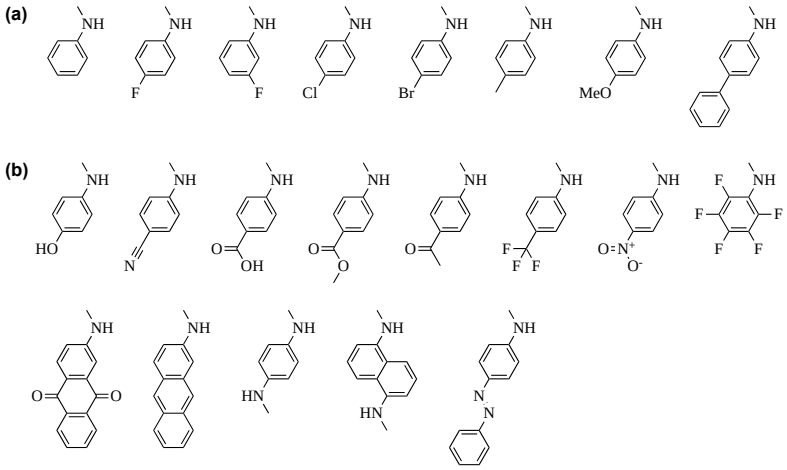

Figure 16. List of molecular structures of organic amine precursors studied, (a) molecules that form 2D hybrid lead halide perovskites persistently, and (b) molecules that failed to form 2D hybrid lead iodide perovskites.

On one hand, methyl ammonium in a 3D hybrid perovskite $MAPbI_3$ seems smaller than the cationic cavity that can be formed in an ideal cubic $APbI_3$ perovskite structure according to the estimated tolerance factor. Relative orientation of MA in $MAPbI_3$ and $RA_2MA_{x-1}Pb_xI_{3x+1}$ varies depend on structures since it's not spherical in shape, and varying hydrogen bonding patterns break symmetry sometimes. On the other hand, $MAPbI_3$ perovskite prepared using lead acetate solution in DMF is shown to incorporate dimethylammonium (DMA) ions in the perovskite lattice. DMA ion is estimated to replace up to 15% of MA in the $MAPbI_3$ structure by NMR spectra, and even with the DMA added in the perovskite lattice, lead iodide scaffold is hardly changed compare to the pure $MAPbI_3$. The N-methyl alkyl ammonium from a secondary amine should be slightly bigger cation in size than primary alkyl ammonium, and known 2D perovskite structures always show "twisted or bended" terminal ammonium groups to compensate the mismatch in size distorting symmetry. Cationic charge center of the N-methyl alky ammonium should be closer to the plane of surface halides with one less hydrogen-bonding than alkyl ammonium known to cause distortion (tilting or twisting) of inorganic layer (**Figure 15a**). The

terminal N-methyl group should limit relative orientation of N-methyl alkyl ammonium potentially simplifying design of other parts of organic cations. Moreover, N-methyl aryl ammonium from an aryl amine should improve design flexibility significantly if the larger ammonium can fit into the anionic cavity especially for organic cations with extended pi-electron conjugation. For example, an aromatic ring conjugated cationic charge center of the N-methyl aryl ammonium should be slightly pushed-out from the inorganic plane and closer to the plane of surface halides with one less hydrogen-bonding similar to N-methyl alkyl ammonium (**Figure 15b**).

In this project, number of 2D hybrid perovskites based on N-methyl aryl ammonium anchor group were synthesized and studied. A list of molecular structures of organic amine precursors studied are summarized in **Figure 16**. They include simple derivatives of N-methyl aniline, N-methyl aromatic compounds with extended conjugation, dicationic N-methyl aromatic compounds, and N-methyl aromatic compounds with stimuli responsive functional groups. Simple derivatives of N-methyl anilinium were studied to understand structure-property relationship and generality, and derivatives with extended conjugation structures were studied to develop 2D hybrid perovskites to construct multi-quantum wells using mixed 2D RPP perovskites.

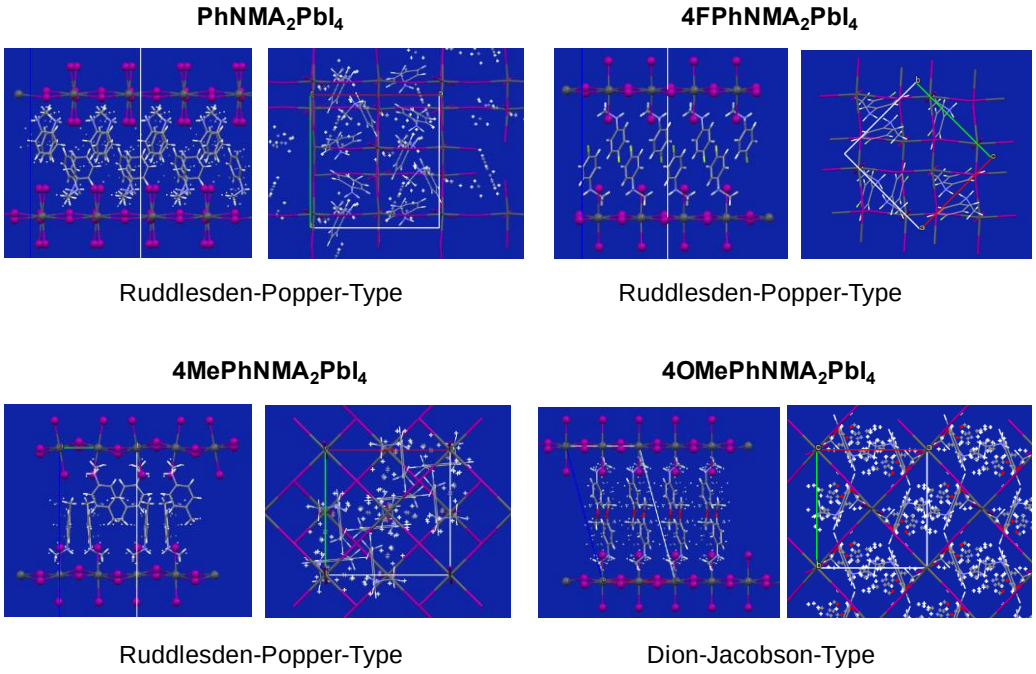

Figure 17. Single crystal x-ray structures of representative examples of 2D hybrid perovskites using the new N-methyl aryl ammonium anchor group showing crystalline phases.

2D perovskites with aryl N-methyl ammoniums can be prepared starting from aryl N-methyl formamide via in situ hydrolysis followed by protonation in acidic solutions. This newly developed procedure can be conveniently applied to prepare high quality crystalline lead halide perovskites via controlled release of precursor cations in solution from formyl group protected N-methyls. High quality crystals of 3D perovskites with methyl ammonium (e.g. $MAPbBr_3$, $MAPbI_3$) can be efficiently prepared by this method also using N-methyl formamide (NMF) as a source of methyl ammonium and processing solvent.

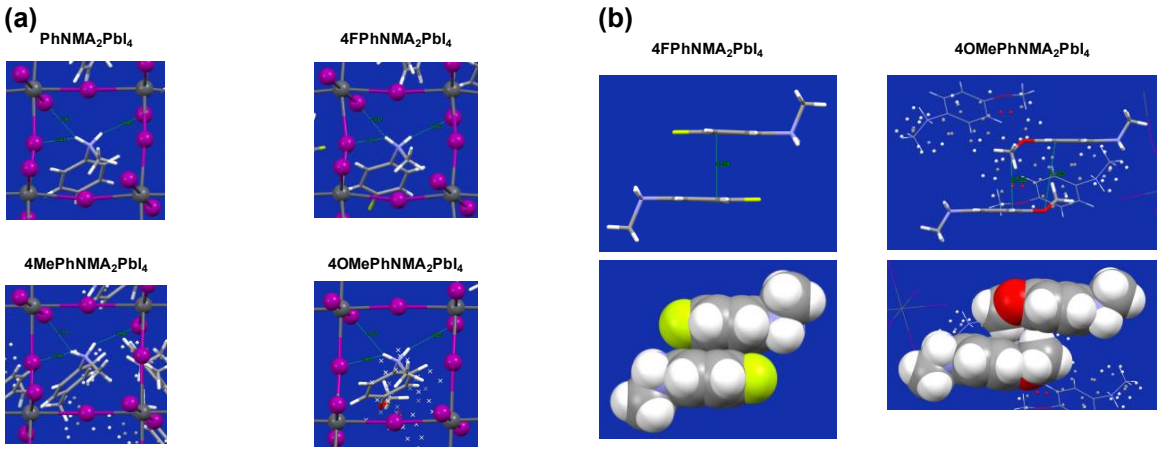

Figure 18. Single crystal x-ray structures of 2D hybrid perovskites of simple derivatives of N-methyl aryl ammonium showing major interactions between (a) organic cations and inorganic layers via three unique hydrogen bondings, and (b) organic cation and organic cations interactions via van der Waals and dipole-dipole interactions.

We have characterized many of prepared 2D hybrid perovskites using single crystal x-ray spectroscopy. Some of representative examples are summarized in **Figure 17**. Nature of interactions between organic and inorganic layers (coulombic, hydrogen bond, halogen-halogen bond) and between organic layers (van der Waals, dipole-dipole) were identified systematically. Due to a lesser number of hydrogen bonds between inorganic layers in perovskites with the secondary N-methyl ammonium group compare to primary ammoniums, the interactions strength appears weaker (or more forgiving) in 2D perovskites between inorganic binding cavity and aryl N-methyl ammoniums compare to perovskites with primary ammoniums. The major intermolecular interactions between organic cations and inorganic layers and organic cations critical for building the 2D hybrid perovskites are summarized in **Figure 18**.

It's still not clear how general are the aryl N-methyl ammonium anchor groups with organic end groups with known non-covalent interactions, variations in confirmation, or potential for in situ hydrolysis (e.g. 4-carboxylic acid, 4-nitro, 4-trifluoromethyl, or 4-cyano phenyl N-methyl ammoniums, **Figure 16b**). The most important factors limiting the generality of the system appear to be strong intermolecular interactions between terminal groups forming the organic layer (e.g. face-to-face, edge-to-edge) in addition to general compatibilities in size and shape of the organics. Relative stabilities of single layer 2D perovskites using 4-fluro phenyl N-methyl ammonium are comparable to PEA based 2D perovskites. However, lead iodide 2D perovskites with 4-fluoro phenyl N-methyl ammonium shows shortest d-spacing among mono-cation system reported (1.37 nm compare to 1.38 nm of 4F-BzA_2PbI_4 and 1.65 nm of PEA_2PbI_4) with full pi-conjugation between cationic center and aromatic group. Crystalline thermal phase transition from and to the lead iodide 2D perovskites were discovered using aryl N-methyl ammoniums. 4-chloro phenyl N-methyl ammonium forms n = 1, lead iodide 2D perovskite phase only at near room temperature. Below 100K, 2D perovskite of lead iodide with 4-methoxy phenyl N-methyl ammonium phase transit to none-2D crystalline phase. Two different conformational factors can be considered to determine such thermochromic phase transition; rotation of terminal functional groups (e.g. 4-methoxy phenyl) and conformational changes of aryl group itself (e.g. 4-chloro phenyl). These are potentially useful for optical sensor applications. Lead iodide n = 1, 2D

perovskites with 4-chloro phenyl and 4-bromo N-methyl ammoniums can be prepared only by the room temperature procedure. Due to the phase transition properties of them, common high temperature preparation method was not applicable for these series. We have also designed and synthesized mono cationic precursor N-methyl aryls and dicationic precursor bis-N-methyl aryls to explore modulation of quantum wells and charge transfer between wells using external stimuli (light, heat, charge). These cations did not form defined 2D perovskite structures.

In summary, we have discovered and studied a completely new class of organic cations based on N-methyl ammonium, N-methyl aryl ammonium in particular as an anchor group that can interact persistently with various metal halides to prepare series of 2D hybrid perovskites. The chemical diversity of 2D hybrid perovskites can be significantly expanded with the discovery, especially the range of possible substitutions on its molecular skeleton that gives an additional structural variability and new functions. Systematic characterizations of developed materials are ongoing.

4.9 Electrically tuanble excitons and many-body interactions

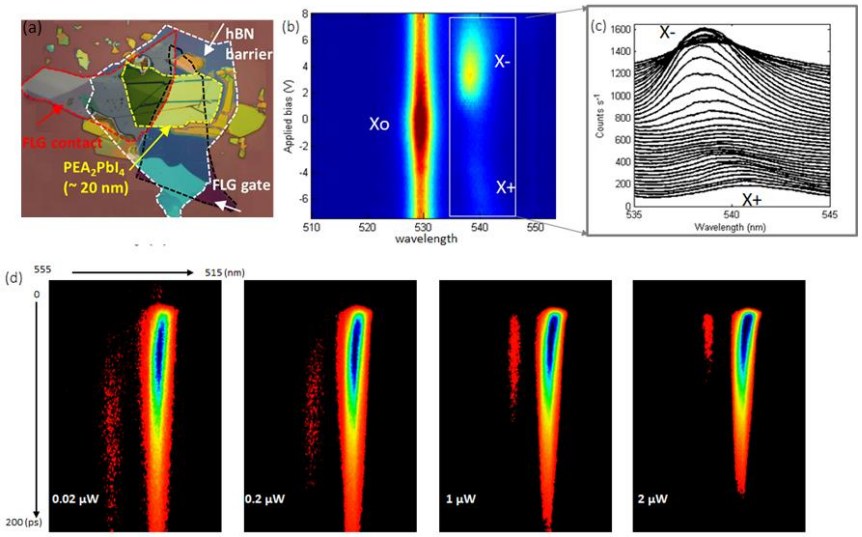

Figure 19. Gate tunable excitons and dynamics. (a) optical microscope image of 2D PEA_2PbI_4 perovskite device. (b) Gate dependent photoluminescence intensity plot of the same device. (c) Zoom in plot of the area in (b) enclosed by the white rectangular box. (d) Time resolved photoluminescence at selected excitation intensity.

There are several outstanding challenges in fabricating 2D perovskite devices for exploring their fundamental properties as well as potential optoelectronic applications. Although as synthesized 2D perovskites crystal are in layered structure and stable, its atomically thin form is still challenge to achieve due to its instability in ambient condition as the thickness approaches a few nm scale. We have developed an all-dry transfer technique to make a sandwiched structure, in which the 2D pervoskite layer is fully encapsulated by the BN layers and is stable in ambient conditions, in the glove box protected by Nitrogen gas. Figure 19a is the optical microscope image of a representative device. This is the first example of gate tunable 2D perovskite device. Using the developed gated sample, we are able to study the excitonic features as a function of carrier doping for the first time. Figure 19b shows the photoluminescence intensity plot as a function of gate voltage. Near zero gate voltage, X^o dominates the photoluminescence spectra.

As the gate voltage is applied, new features emerge. Negatively (X^-) and positively (X^+) charged excitons appear in the electron (positive gate) and hole (negative gate) regimes (Figure 19c), respectively. This study clarifies the origin of the photoluminescence features and established 2D

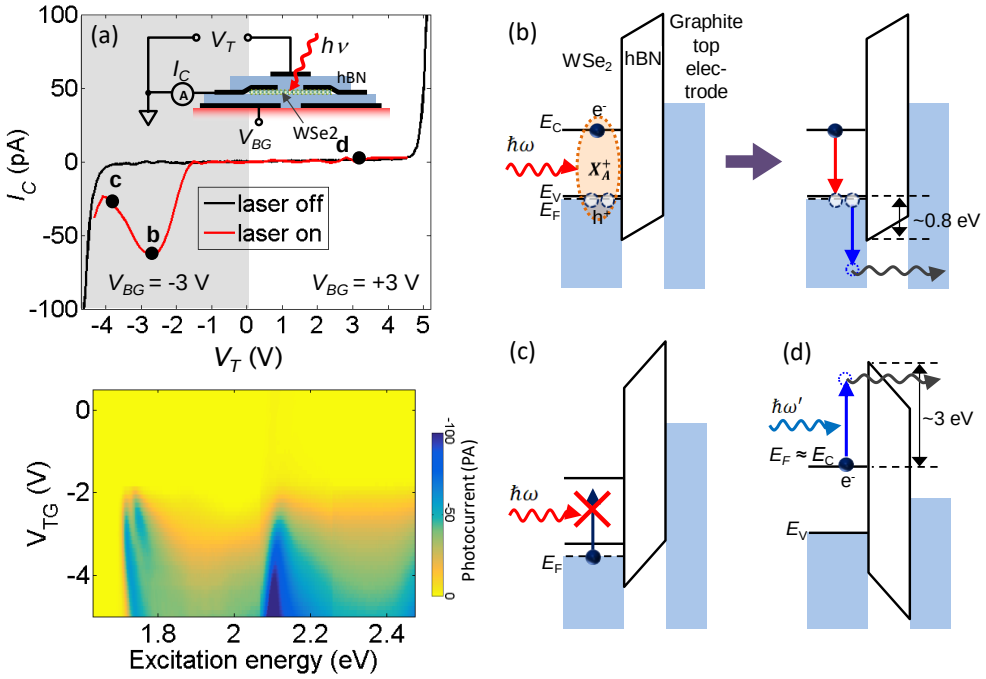

Figure 20. Auger photocarrier detection. (**a**) Top: Gate current (I_C) between a contact and top electrode (T) versus V_T with (red) and without (black) laser illumination at $\hbar\omega$ = 1.71 eV (1 μW at 725 nm). Inset: schematic of device and experiment. Bottom: Intensity plot of photocurrent I_C as a function of V_T and excitation energy (at $V_{BG} = -3$ V). (**b**) When V_T is negative the WSe_2 is p-doped. At a certain value of V_T (point **b** in I_C versus V_T plot), ω is in the middle of the positive trion X_A^+ absorption resonance and X_A^+ trions are most rapidly created (left panel). Recombination of an electron and hole in a trion causes Auger scattering of the remaining hole to an energy below the hBN valence band edge, allowing it to pass through the hBN producing photocurrent (right panel). (**c**) As V_T is made more negative (point **c**), the X_A^+ resonance blue-shifts, causing the rate of creation of excitons and hence the photocurrent to decrease. (**d**) When V_T is positive the WSe_2 is n-doped. The large conduction band offset here prevents photoexcitation directly over the barrier, but at large enough V_T (point **d**) photo-excited electrons can tunnel across the hBN barrier.

perovskites as a new tunable quantum well platform.

We further investigated the dynamics of excitons using time resolved photoluminescence spectroscopy. A state-of-the-art streak camera with 1 ps time resolution is used for this study. The experiment is done at 2K. We excite the sample with 150 fs laser pulses at 480 nm. Figure 19d shows the time resolved measurements at four selected excitation power. This measurement observe two remarkable phenomena. As we increase the exciton power, there are significant red shift of X^o energy as a function of time. This observation implies strong exciton exciton interactions near time zero, signature of reduced screen effects at the atomically thin limit. In addition, the energy transfer from neutral and charged excitons significantly enhanced as the excitation power. The peak intensity of charged exciton changes from 100 ps to 10 ps as the

excitation power increased from 20 nw to 2 μW. The dynamics of exciton also involves many-body interaction effcts, such as Auger scattering. Auger scattering is a ubiquitous phenomenon in photoexcited semiconductors, especially in low dimensional materials where reduced Coulomb screening enhances many-body interactions. Directly probing Auger scattering in solid state devices is a known challenge because Auger processes are ultrafast and nonradiative.

Nonetheless, it can offer important insights on photocarrier dynamics and many-body interactions, which are among primary considerations for a wide range of optoelectronic and photovoltaic applications. During this award period, we demonstrate a new concept to directly probe Auger scattering with a commonly used van der Waals device geometry, consisting of a monolayer quantum well WSe_2 as the photo-active semiconductor, a thin hexagonal boron nitride (hBN) dielectric barrier, and a few-layer graphene gate/electrode (Figure 20). The wide band gap hBN functions as an energy filter, allowing high energy Auger carriers in WSe_2 to reach the graphite electrode, while blocking the low energy carriers. Auger carriers are thus detected as photocurrent across the gate and contact electrodes. This approach leads to our uncovering of an important Auger mechanism between hole and several excitonic species. The Auger rate here is estimated to be two orders of magnitude higher than that in 3D bulk semiconductors due to stronger carrier-carrier interaction in 2D systems.

Our finding is supported by multiple observations. First, the association between Auger photocurrent and optical absorption peaks evinces the excitonic origin of the aforementioned Auger process. Second, linear scaling of the Auger photocurrent with respect to laser excitation intensity rules out exciton-exciton Auger as the dominant mechanism. Third, the absence of Auger photocurrent in electron-doped regime at low photoexcitation energy, as well as the emergence of photocurrent at specific gate bias and excitation energy range, is consistent with known band offsets between WSe2 and hBN. The dependence of Auger photocurrent on both excitation energy and bias gives rise to negative differential photoconductance. This can potentially serve as a novel spectroscopic technique to probe the interplay between valence band filling and renormalization of exciton energies. Our work demonstrates a new way to directly probe evasive Auger scattering, which will be applied into study gated 2D perovskites, as we developed in year 1.

5. Publications

1) "Monolayer Semiconductor Auger Detector, Colin M. Chow, Hongyi Yu, John R. Schaibley, Pasqual Rivera, Joseph Finney, Jiaqiang Yan, David G. Mandrus, Takashi Taniguchi, Kenji Watanabe, Wang Yao, David H. Cobden, Xiaodong Xu", **Nano Letters,** https://pubs.acs.org/doi/10.1021/acs.nanolett.0c02190 (2020).
2) "Regulating surface termination for efficient inverted perovskite solar cells with greater than 23% efficiency", F. Li, X. Deng, F. Qi, Z. Li, D. Liu, D. Shen, M. Qin, S. Wu, F. Lin, S.-H. Jang, J. Zhang, X. Lu, D. Lei, C.-S. Lee, Z. Zhu, and A. K.-Y. Jen, ***J. Am. Chem. Soc.***, 142, 20134 (2020).

6. Patent.

"Perovskites materials incorporating N-methyl aryl cations", S.-H. Jang, A. K.-Y. Jen, *U.S. Provisional Patent Application* 63050674, July, **2020**.